

Entanglement in Correlated Fermionic Systems and Quantum Phase Transitions

Alberto Anfossi¹, Paolo Giorda^{1,2}, and Arianna Montorsi¹

¹ Dipartimento di Fisica del Politecnico and CNISM, C.so Duca degli Abruzzi 24, I-10129 Torino, Italy and

² Institute for Scientific Interchange (ISI), Villa Gualino, Viale Settimio Severo 65, I-10133 Torino, Italy

(Dated: December 2, 2024)

The role of two-point and multipartite entanglement at Quantum Phase Transitions (QPTs) in correlated electron systems is investigated. We consider a bond-charge extended Hubbard model exactly solvable in one dimension which displays various QPTs –with two (qubits) as well as more (qudits) on-site degrees of freedom involved. We first provide the detailed calculations that allow to classify the QPTs according to 10. The analysis is then carried out by means of different measures of bipartite/multipartite quantum correlations. It is found that all transitions ascribed to two-point correlations are characterized by an entanglement range which diverges at the transition points. The exponent coincides with that of the correlation length at the transitions. We introduce the Correlation Ratio, namely the ratio of quantum mutual information and single site entanglement. We show that at $T = 0$ it captures the relative role of two-point and multipartite quantum correlations at transition points, generalizing to qudits systems the Entanglement Ratio. Moreover, a finite value of quantum mutual information between infinitely distant sites is seen to quantify the presence of off diagonal long range order (ODLRO) induced by multipartite entanglement.

PACS numbers: 03.67.Ud, 71.10.-w

I. INTRODUCTION

In the past years, the characterization of complex quantum phenomena has received an impulse from the recent developments in quantum-information theory. Within such framework an important notion is that of entanglement between subsystems. Besides being recognized as a fundamental resource for quantum computation and communication tasks¹, it has also been used to better characterize the critical behavior of different many-body quantum systems undergoing quantum phase transitions (QPTs)².

The large amount of results achieved^{3–12} relies on the observation that a QPT is in general characterized through non-analyticities of the density matrix of an appropriate subsystem. The latter is the starting point for any measure of entanglement –*i.e.* quantum correlation– either within the subsystem or between the subsystem and the remaining system. In the latter case Von Neumann entropy S is always able to capture the presence of a QPT (of finite order) for appropriate choice of the subsystem. Also, some general information about the type of transition (for instance its order) can be gained by looking at the type of singularity in S^5 . Nevertheless, in order to construct a complete description of QPTs, one should provide a plethora of other features, such as, for instance, critical exponents. This requires the evaluation of more punctual measures of entanglement, like that of quantum correlations between two points; or among more subsystems (multipartite correlations). Such measures have been already investigated in relations to QPTs for qubits systems. In 3 it was shown that Concurrence (measuring two-point entanglement) scales with universal exponent for an XY model. Whereas in 6 the n -tangle measure was used to detect the singular behavior of multipartite correlations at a QPT.

A certain number of interesting results has been obtained as well for QPTs and entanglement for *correlated electron systems*^{9–12}, the latter being in principle characterized by a larger number of degrees of freedom per site (typically four)

with respect to qubits systems. This point makes it necessary to use measures of quantum correlations which are tailored also for qudits systems. Most of such measures are difficult to evaluate whenever the subsystem is in a mixed state, since they require an –often out of reach– optimization process. In 10 a method was proposed to distinguish at a given QPT the contribution of two-point entanglement from that of multipartite quantum correlations without entering the above difficulties. The method is based on the comparative use of single site Von Neumann entropy S_i and quantum mutual information I_{ij} , the latter being a measure of all (quantum and classical) correlations between two generic sites i, j . The method provides a simple recipe: whenever the two measures display the same type of singularity at a given transition, the latter is to ascribe to two-point correlations; on the contrary, if the singularity displayed by S_i is seen differently by I_{ij} , the transition is to ascribe to multipartite correlations.

In the present paper we first review the above method, deriving in details the results at $T = 0$ for an extended Hubbard model which is exactly solvable in one dimension. Then we compare such results with those obtained by using measures of two-point/multipartite quantum correlations developed recently in quantum information, with particular emphasis on Negativity²⁰, Concurrence¹⁹ and Entanglement Ratio⁶. In particular, in order to generalize the latter to qudits systems the Correlation Ratio is introduced. Also, the relation between critical exponents at the transitions and scaling behavior of the entanglement measure at those critical points is studied.

The plan of the paper is the following. In Section II we introduce the model and its exact solution; we also derive the one- and two-site reduced density matrices. In Section III we describe different measures of bipartite/multipartite correlations for qubits and qudits systems. In section IV we present and discuss the results obtained for the various measures at the different metal-insulator-superconducting transitions which characterize the model. Finally, in section V we summarize our main conclusions.

II. THE BOND-CHARGE EXTENDED HUBBARD MODEL

The model is described by the Hamiltonian:

$$H_{BC} = - \sum_{\langle i,j \rangle \sigma} [1 - x(n_{i\sigma} + n_{j\sigma})] c_{i\sigma}^\dagger c_{j\sigma} - \mu \sum_{i\sigma} n_{i\sigma} + u \sum_i (n_{i\uparrow} - \frac{1}{2})(n_{i\downarrow} - \frac{1}{2}), \quad (1)$$

where $c_{i\sigma}^\dagger, c_{i\sigma}$ are fermionic creation and annihilation operators on a one-dimensional chain of length L ; $\sigma = \uparrow, \downarrow$ is the

spin label, $\bar{\sigma}$ denotes its opposite, $n_{j\sigma} = c_{j\sigma}^\dagger c_{j\sigma}$ is the spin- σ electron charge, and $\langle i, j \rangle$ stands for neighboring sites on the chain; u and x ($0 \leq x \leq 1$) are the (dimensionless) on-site Coulomb repulsion and bond-charge interaction parameters; μ is the chemical potential, and the corresponding term allows for arbitrary filling.

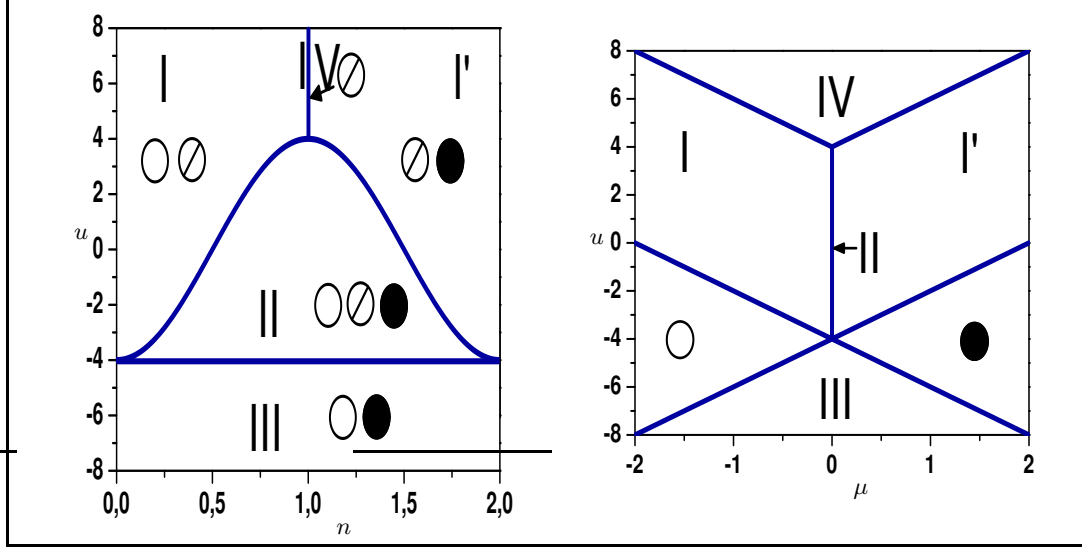


FIG. 1: Ground state phase diagram of H . LEFT: n - u plane; empty circles stand for empty sites, slashed and full circles stand for singly and doubly occupied sites respectively; RIGHT: μ - u plane.

The model is considered here at $x = 1$, in which case the number of doubly occupied sites becomes a conserved quantity, and the role of spin orientation becomes to many aspects irrelevant: for an open chain any sequence of spins in the chain cannot be altered by the Hamiltonian, whereas for periodic boundary conditions only the sequences of spins related by a cyclic permutation can be obtained. In particular, the ground state turns out to be degenerate with the fully polarized state, and the system behaves as if at each site i the local space had dimension $D_i = 3$. In practice, both the Hamiltonian and the local vector space can be written in terms of the new Hubbard projection operators $X_i^{\alpha\beta} \doteq |\alpha\rangle_i\langle\beta|_i$, with local algebra $X_i^{\alpha\beta} X_j^{\gamma\delta} = \delta_{\beta\gamma} X_i^{\alpha\delta}$ and non local (anti-)commutation relations given by

$$X_i^{\alpha\beta} X_j^{\gamma\delta} = (-)^{(\alpha+\beta)(\gamma+\delta)} X_j^{\gamma\delta} X_i^{\alpha\beta} \quad i \neq j; \quad (2)$$

here $\alpha = 0, 1, 2$, $|0\rangle_i \equiv |\text{vac}\rangle_i$ is the local vacuum, $|1\rangle_i \doteq X_i^{10}|0\rangle_i$ is the singly occupied state (with odd parity), and $|2\rangle_i \doteq X_i^{20}|0\rangle_i$ is the doubly occupied state. More precisely, as far as the ground state is concerned, the model Hamiltonian in the 1-dimensional case can be fruitfully written as

$$H = - \sum_i (X_i^{10} X_{i+1}^{01} - X_i^{21} X_{i+1}^{12} + h.c.) + u \sum_i X_i^{22} - \left(\mu + \frac{u}{2} \right) \sum_i (X_i^{11} + 2X_i^{22}), \quad (3)$$

In this form H provides the full spectrum of H_{BC} at $x = 1$ for open boundary conditions, and its full ground-state phase diagram for both open and periodic boundary conditions.

A. Spectrum and ground-state phase diagram

The physics of the system described by H is basically that of $N_s = \langle \sum_i X_i^{11} \rangle$ spinless fermions which move in a background of $L - N_s$ bosons of which $N_d = \langle \sum_i X_i^{22} \rangle$ are doubly occupied sites and the remaining are empty sites. Both N_s and N_d are conserved quantities, and determine the total number of electrons $N = N_s + 2N_d$.

The situation may be understood in the formalism developed by Sutherland in 13. We can say that, apart from constant terms, H acts as a permutator of just two *Sutherland species*(SSs), the N_s fermions and the $L - N_s$ bosons. In practice, empty and doubly occupied states –though different as physical species– belong to the same SS, since the off-diagonal part of the Hamiltonian can not distinguish between them. It is only the constant term counting doubly occupied sites which depends on the actual value of N_d .

The eigenstates are easily worked out^{14,15}, and read

$$|\psi(N_s, N_d)\rangle = \mathcal{N}(\eta^\dagger)^{N_d} \tilde{X}_{k_1}^{10} \cdots \tilde{X}_{k_{N_s}}^{10} |\text{vac}\rangle; \quad (4)$$

the result holding also at finite L if periodic boundary conditions are chosen in (3). Here

$$\mathcal{N} = \left[(L - N_s - N_d)! / (L - N_s)! N_d! \right]^{1/2}$$

is a normalization factor; \tilde{X}_k^{10} is the Fourier transform of the Hubbard projection operator X_j^{10} i.e. $\tilde{X}_k^{10} =$

$\sum_j \frac{1}{\sqrt{L}} \exp(i \frac{\pi}{L} j k) X_j^{10}$. Moreover $\eta^\dagger = \sum_{i=1}^L X_i^{20}$ is also known as the eta operator, commuting with H ; $(\eta^\dagger)^{N_d}$ creates N_d pairs (or doubly occupied sites).

The actual ground state $|\psi_{GS}(N_s, N_d)\rangle$ is chosen among the eigenstates in (4) by requiring that N_s and N_d minimize the corresponding eigenvalue

$$E(N_s, N_d) = -2 \frac{L}{\pi} \sin(\pi \frac{N_s}{L}) + u N_d - \mu(N_s + 2N_d).$$

In Fig. 1, we report on the right the ground state phase diagram in the n - u plane (with $n = N/L$ average per-site filling); in the left part, the same diagram in the μ - u plane. The phase diagram presents various QPTs driven by parameters u and μ (or n). Tab. I gives the range of parameters characterizing each phase in the thermodynamic limit ($L, N_\alpha \rightarrow \infty$, with $n_\alpha = N_\alpha/L$ finite). Each transition is characterized by a change in the number of on-site degrees of freedom (d.o.f.) involved in the state. Phase IV has just one d.o.f. per site since each site is singly occupied; it is an insulating phase, with charge gap $\Delta_c^{(IV)} = \mu_+ - \mu_- = u - 4$, where μ_+ (μ_-) is the energy cost for adding (removing) one electron. Phases I and I' (which is the particle-hole counterpart of phase I) have two on-site d.o.f.: singly occupied sites, and empty or doubly occupied sites respectively. This holds for phase III as well, where only empty and doubly occupied sites appear. Phase II is the only phase in which all three on-site d.o.f. are involved.

Region of the Phase Diagram	u	μ	GS Energy
$I : n_s = n$ $n_d = 0$	$u > u_c(n)$	$\mu = -2 \cos \pi n - u/2$	$-2/\pi \sin(\pi n)$
$I' : n_s = 2 - n$ $n_d = n - 1$	$u > u_c(n)$	$\mu = 2 \cos \pi n + u/2$	$-2/\pi \sin(\pi n) + u(n - 1)$
$II : n_s = 1/\pi \arccos(-u/4)$ $n_d = 1/2(n - n_s)$	$u \in [-4, u_c(n)]$	$\mu = 0$	$-2/\pi \sqrt{1 - (u/4)^2} + u/2[n - 1/\pi \arccos(-u/4)]$
$III : n_s = 0$ $n_d = n/2$	$u < -4$	$\mu_\pm = \mp(2 + u/2)$	$un/2$
$IV : n_s = n = 1$ $n_d = 0$	$u > 4$	$\mu_\pm = \mp(2 - u/2)$	0

TABLE I: Ground state sectors and corresponding energies; here $u_c(n) \doteq -4 \cos(\pi n)$. Notice that the values limiting the range of u and/or μ in each sector are the critical values for the transitions

Notice that, as far as the relevant physics is concerned, this seems to be related to the number of on-site SSs characterizing the phase rather than the number of on-site d.o.f. In fact, phase I , I' and II –which all have both the bosonic and

the fermionic SS– fall in the Tomonaga-Luttinger class, since neither spin nor charge gap are present. Whereas phase III , though characterized by empty and doubly occupied states, has just the bosonic SS; it is again insulating, with charge gap

$$\Delta_c^{(III)} = -u - 4.$$

Despite the above observation, phases I , I' differ from phase II since only the latter is characterized by the occurrence of Off-Diagonal Long Range Order (ODLRO) and superconducting correlations (which also survive in phase III):

$$\lim_{r \rightarrow \infty} \langle X_i^{20} X_{i+r}^{02} \rangle = n_d(1 - n_d). \quad (5)$$

Notice that ODLRO –though not allowing real superconducting order at $x = 1$ due to spin degeneracy, which implies absence of spin gap⁽¹⁶⁾– is at the very root of superconducting order which occurs at any $x \neq 1$ ⁽¹²⁾.

Before discussing the various transitions in terms of the behavior of entanglement measures, let us recall some feature of each of them in terms of standard theory.

First of all, since N_d and N_s are both conserved quantities, the transitions should be originated from level crossing. Indeed, they also occur at finite L . Nevertheless, none of them is of first order, since it can be easily checked from Tab. (I) that the first derivative of E_{GS} is always smooth.

Second, N_s ($1 - N_s$) and N_d ($1 - N_d$) can also be considered as order parameters for the transitions, since all of QPTs occur in correspondence of the vanishing of one or both the above quantities.

Moreover, all the three transitions $I \rightarrow IV$, $II \rightarrow III$ and $II \rightarrow IV$ correspond to the opening of an insulating phase, characterized by a charge gap linear in u (and in μ). This implies that the product of the dynamical exponent z and the critical exponent ν of the correlation length is one for all the three transitions. Furthermore, since $\rho = (d+z)\nu - 1$, with ρ exponent characterizing the first derivative of the free-energy, we obtain that all of the three above transitions have $\nu = 1/2$, $z = 2$.

The situation is less clear at the transition $II \rightarrow I, I'$, since on the one hand no spin nor charge gap open in both phases. On the other hand it must be said that N_d , and consequently η -pairs and ODLRO, vanish in correspondence of the transition. This is true as well for the pairing gap Δ_P , $\Delta_P = E(N+2) + E(N) - 2E(N+1)$. Indeed it can be seen that $\Delta_P = 0$ in phase I , and $\Delta_P = u - u_c(n) < 0$ in phase II , where $u_c(n)$ defines the critical line.

B. Reduced density matrices

The evaluation of the measures of correlation described in the following sections requires the manipulation of the single-site and dimer reduced density matrix, ρ_i and ρ_{ij} . These can be obtained from the system density matrix in the ground state, the latter being defined as usual by $\rho_{GS} \doteq |\psi_{GS}\rangle\langle\psi_{GS}|$. The reduced density matrix ρ_i (ρ_{ij}) is then the trace of ρ_{GS} with respect to all the d.o.f. except those of the site i (sites i, j). These matrices can be constructed in a simple way from the one- and two-point correlation functions, using the *operator expansion* for the density matrix in terms of the Hubbard projectors (2); one has however to pay attention to the existing graded structure of the fermionic algebra¹⁷, see App. A). In particular, the one-site reduced density matrix can be written

as

$$\rho_i = Tr_{L/i}(\rho_{GS}) = \sum_{\alpha, \beta=0,1,2} q_{\alpha\beta} X_i^{\alpha\beta},$$

where $q_{\alpha\beta} = \langle \psi_{GS} | X_i^{\alpha\beta} | \psi_{GS} \rangle$, while the two-site reduced density matrix reads

$$\rho_{ij} = Tr_{L/\{ij\}}(\rho_{GS}) = \sum_{\alpha, \beta, \gamma, \delta=0,1,2} q_{\alpha\beta\gamma\delta} X_i^{\alpha\beta} X_j^{\gamma\delta},$$

$$\text{with } q_{\alpha\beta\gamma\delta} = \langle \psi_{GS} | X_i^{\alpha\beta} X_j^{\gamma\delta} | \psi_{GS} \rangle.$$

Below we report the results for ρ_i and ρ_{ij} (the detailed derivation of the calculations for the dimer case can be found in Appendix B).

When expressed in terms of the basis $\{|0\rangle_i, |1\rangle_i, |2\rangle_i\}$ ρ_i is diagonal in all the regions of the phase diagram:

$$\rho_i = \text{diag} \{1 - n_s - n_d, n_s, n_d\} \quad , \quad (6)$$

whereas with respect to the basis $\{|00\rangle, |01\rangle, |10\rangle, |11\rangle, |12\rangle, |21\rangle, |02\rangle, |20\rangle, |22\rangle\}$ ρ_{ij} reads

$$\rho_{ij} = \begin{pmatrix} D_1 & 0 & 0 & 0 & 0 & 0 & 0 & 0 & 0 \\ 0 & O_1 & O_2 & 0 & 0 & 0 & 0 & 0 & 0 \\ 0 & O_2^* & O_1 & 0 & 0 & 0 & 0 & 0 & 0 \\ 0 & 0 & 0 & D_2 & 0 & 0 & 0 & 0 & 0 \\ 0 & 0 & 0 & 0 & P_1 & P_2 & 0 & 0 & 0 \\ 0 & 0 & 0 & 0 & P_2^* & P_1 & 0 & 0 & 0 \\ 0 & 0 & 0 & 0 & 0 & 0 & Q & Q & 0 \\ 0 & 0 & 0 & 0 & 0 & 0 & Q & Q & 0 \\ 0 & 0 & 0 & 0 & 0 & 0 & 0 & 0 & D_3 \end{pmatrix}. \quad (7)$$

Here

$$\begin{aligned} D_1 &= P_{ij}(1 - c)^{\frac{1-c-\epsilon}{1-\epsilon}} & O_2 &= \Gamma_{ij}(1 - c) \\ D_2 &= n_s^2 - |\Gamma_{ij}|^2 & P_1 &= c(1 - n_s - P_{ij}) \\ D_3 &= c\frac{c-\epsilon}{1-\epsilon} P_{ij} & P_2 &= c\Gamma_{ij} \\ O_1 &= (1 - n_s - P_{ij})(1 - c) & Q &= \frac{c(1-c)}{1-\epsilon} P_{ij} \end{aligned}$$

with $c = n_d/(1 - n_s)$, $P_{ij} = (1 - n_s)^2 - |\Gamma_{ij}|^2$, $\epsilon = c/L$ and

$$|\Gamma_{ij}| = \frac{1}{L} \frac{\sin(n_s \pi |i - j|)}{\sin(\frac{\pi}{L} |i - j|)}.$$

III. MEASURES OF ENTANGLEMENT

The theory of quantum information has provided the study of complex quantum phenomena, such as QPTs, of new and well defined tools. In many cases these tools have been used to describe the (critical) behaviour of relevant many-body systems. In some relevant cases they also provide more detailed information, such as critical exponents or type of quantum correlations involved.

In general, the fact that a critical behavior can be spotted by appropriate measures of entanglement should not be a surprise

from the point of view of Landau theory since any measure of entanglement can be expressed as a unique functional of first derivatives of the ground-state energy⁵. Nevertheless, the use of more advanced tools could provide new interesting features difficult to extract from standard theory. For instance, in 10 we have described how, by using the appropriate measures of bipartite correlations, it is possible not only to fully describe the phase diagram of some model, but also to discriminate the role of two-point from that of multipartite entanglement at each of the QPTs the system undergoes.

A. Separating two-point from multipartite entanglement at QPTs

In this section we briefly recall the method used in 10 where we were interested in the existing correlations between: *a*) the single site i and the rest of the system; *b*) the generic site i and a generic site $j \neq i$.

Since the full system is in a pure (ground) state, the amount of quantum correlations between a single site and the rest of the system is measured by the Von Neumann entropy of ρ_i :

$$\mathcal{S}_i = \mathcal{S}(\rho_i) = - \sum_{j=1}^D \lambda_j \log_2 \lambda_j \quad , \quad (8)$$

where λ_j , $j = 1, \dots, D$ are the eigenvalues of the reduced density matrix ρ_i .

The total correlations (quantum and classical) between two sites i, j are captured by the quantum mutual information:

$$\mathcal{I}_{ij} = \mathcal{S}(\rho_i) + \mathcal{S}(\rho_j) - \mathcal{S}(\rho_{ij}) , \quad (9)$$

where $\mathcal{S}(\rho_{ij})$ is the two-site Von Neumann entropy, $\mathcal{S}(\rho_{ij}) = \sum_{j=1}^{D^2} \tilde{\lambda}_j \log_2 \tilde{\lambda}_j$, and $\tilde{\lambda}_j$, $j = 1, \dots, D^2$ are the eigenvalues of ρ_{ij} .

To resume, we have the following situation. On the one hand, the single site is quantum correlated with the rest of the system in two possible way: via two-point correlations (*Q2*), when it is "individually" correlated with some/all the other sites; via multipartite correlations (*QS*), when it is connected through n -point quantum correlations. On the other hand, the mutual information allows one to evaluate all the correlations connecting two sites; the latter can be of a quantum nature, the already mentioned *Q2*, and/or of a classical nature (*C2*). While the Single-site Entanglement $\mathcal{S}(\rho_i)$ is not able to distinguish between *Q2* and *QS*, the mutual information \mathcal{I}_{ij} is not able to distinguish between *Q2* and *C2*. Nevertheless, in 10, we have shown that a comparison of the singular behavior of \mathcal{S}_i with that of \mathcal{I}_{ij} allows one to discriminate whether a QPT is to ascribe to *Q2* or *QS* correlations. In fact, whenever the singular behaviour exhibited by \mathcal{S}_i is due to *Q2* correlations, the *same* type of singular behavior is necessarily displayed by \mathcal{I}_{ij} as well, since it also contains *Q2* correlations.

B. Measuring two-point entanglement

The task of measuring quantum correlations between two given sites i and j has a simple solution when i and j are two-level systems (qubits) in terms of the *Concurrence*¹⁹. Even when i and j are arbitrary qudits the quantification of entanglement can be carried on by means of the *Negativity*. Notice that the latter is a lower bound of Concurrence²¹ and fails to signal the entanglement in the sub-set of mixed states called Partial Positive Transpose states.

1. Concurrence

The Concurrence was first introduced in 19 and, for the case of two qubits, it is directly related to the entanglement of formation. In order to evaluate the Concurrence one has to first manipulate the two qubits density matrix ρ_{ij} and find $\tilde{\rho}_{ij} = \rho_{ij} \sigma_y \otimes \sigma_y \rho_{ij}^* \sigma_y \otimes \sigma_y$ where ρ_{ij}^* is the element-wise complex conjugate of ρ_{ij} . The Concurrence can then be written as

$$\mathcal{C}(\rho_{ij}) = \max\{0, \lambda_1 - \lambda_2 - \lambda_3 - \lambda_4\} \quad (10)$$

where the λ_i 's are the square roots of the eigenvalues of $\tilde{\rho}_{ij}$ taken in decreasing order.

2. Negativity

Another measure of bipartite quantum correlations *Q2* used in 10 is the Negativity

$$\mathcal{N}_{ij} = \mathcal{N}(\rho_{ij}) = (\|\rho_{ij}^{T_i}\|_1 - 1)/(D - 1); \quad (11)$$

where $\rho_{ij}^{T_i}$ is the partial transposition with respect to the subsystem (site) i applied on ρ_{ij} , and $\|O\|_1 \doteq \text{Tr} \sqrt{O^\dagger O}$ is the trace norm of the operator O . $\rho_{ij}^{T_i}$ can have negative eigenvalues μ_n and the Negativity can also be expressed as $\mathcal{N}(\rho_{ij}) = |\sum_n \mu_n|$. Although the Negativity is not a perfect measure of entanglement²⁹, it gives important bounds for quantum information protocols *i.e.*, teleportation capacity and asymptotic distillability.

One would reasonably expect the measures of two-point entanglement to exhibit the same singular behaviour of \mathcal{S}_i and \mathcal{I}_{ij} when the transitions are to ascribe to *Q2* correlations. The analysis performed in 10, and deepen in this paper, shows that this is not always the case. To understand such an unexpected feature we shall explore in more details the behavior of both \mathcal{N}_{ij} and \mathcal{C}_{ij} when $|i - j|$ is varied in proximity of the QPTs dominated by *Q2* correlations.

C. Multipartite entanglement measurements

The case in which the singular behavior of \mathcal{S}_i is to ascribe to *QS* correlations can also be treated with the described bipartite measures in a simple, though not complete way. The only

thing that one can say is that when the QS enter into play, the same singular behavior should not be displayed neither by \mathcal{I}_{ij} , nor by \mathcal{N}_{ij} , since both measures regard only two-point correlations.

In order to refine and confirm our analysis we now proceed to a review of the available measures for multipartite entanglement that have been developed recently.

1. Residual entanglement: the tangle

The idea of *residual entanglement* was first introduced in 22 where the case of a three qubits system in a pure state $|\psi_{ABC}\rangle$ was studied. Here are the basis ideas:

i) the Concurrence for a *two qubit pure state* reduces to:

$$\mathcal{C}_{A,B} = 2\sqrt{\det \rho_A} \quad (12)$$

ii) once a *focus* qubit is chosen, in this case A , the following inequality holds for a *three qubit pure state*:

$$4\det \rho_A \geq \mathcal{C}_{AB}^2 + \mathcal{C}_{AC}^2 \quad (13)$$

iii) in the case of *three qubit pure state*, the subsystem constituted by the pair (B, C) is four dimensional but only two of these dimensions can be used to express the state; in other words both the reduced density matrices ρ_A and ρ_{BC} have only two non zero eigenvalues. This fact leads to interpret $2\sqrt{\det \rho_A}$ as the Concurrence between A and (B, C) and thus to rewrite the above inequality as:

$$\mathcal{C}_{A,(BC)}^2 \geq \mathcal{C}_{AB}^2 + \mathcal{C}_{AC}^2. \quad (14)$$

The last result says that the entanglement that the focus qubit A can establish with each of the other qubits separately is bounded by the entanglement that it can globally establish with them. (The latter is a property that is not satisfied by the entanglement of formation). The definition of RE for *three qubit pure state*, or *tangle*, can be introduced in the following unique way on the basis of the above results and of the fact that they do not depend on the focus qubit chosen:

$$\tau_{ABC} = \mathcal{C}_{A,(BC)}^2 - \mathcal{C}_{AB}^2 - \mathcal{C}_{AC}^2. \quad (15)$$

Due to the permutation invariance, this quantity properly measures at least an aspect of three-qubit entanglement: the *three-way entanglement*.

2. Entanglement Ratio

An example of the use of the *tangles* for the exploration of QPTs in spin systems is given in 6. There, in order to detect the relevance of the two-point versus the n -way entanglement ($n > 2$) the “CKW-conjecture” was assumed, *i.e.* the *conjecture* that the inequality (14) can be extended to states of an arbitrary number of qubits²²:

$$\tau_1 = \mathcal{C}_{A,(BC..N)}^2 \geq \mathcal{C}_{AB}^2 + \mathcal{C}_{AC}^2 + \dots + \mathcal{C}_{AN}^2 = \tau_2. \quad (16)$$

Notice that for spin systems all the concurrences can be easily evaluated due to the qubit nature of the subsystems.

In 6, starting from the above conjecture, the authors define the *Entanglement Ratio* E_R :

$$E_R = \tau_2 / \tau_1 < 1. \quad (17)$$

The more the ratio decreases, the more QS correlations are relevant with respect to $Q2$ ones.

Recently the “CKW-conjecture” has been rigorously proven in 23.

Generalizations of the above results were carried out in 25,26 where the authors provided the generalization of *bipartite* entanglement measure in the case of *arbitrary dimensions* of the subsystems and defined –even in this case– the notion of “tangle”. The latter construction is in general difficult to apply, since the determination of the generalized bipartite Concurrence requires application of optimization processes. In our case this implies that the the Entanglement Ratio can be easily applied only in the phase where the local Hilbert space is of a two qubits kind *i.e.*, in phase *I* and *III*.

In order to overcome this problem and study the transition $II \rightarrow I, III, IV$ we will make use of a different kind of ratio that allows one to compare the *total* two-point correlations with the total correlations (quantum) of a single site with respect to the others.

This can be done by substituting in the definition of the Entanglement Ratio: i) the sum of the squares of two sites Concurrences τ_2 with the sum of quantum mutual information \mathcal{I}_{ij} *i.e.*

$$\tilde{\tau}_2 = \sum_{j=1}^{L-1} \mathcal{I}_{ij}; \quad (18)$$

ii) the linear entropy τ_1 with the Single-site Entanglement $\tilde{\tau}_1 = \mathcal{S}_i$. The new ratio –termed Correlation Ratio– reads

$$C_R = \tilde{\tau}_2 / \tilde{\tau}_1. \quad (19)$$

The fact that quantum correlations cannot be freely shared by many object is encoded in the so-called monogamy principle demonstrated in 23, which is at the base of the definition of τ_2 . Classical correlations $C2$ are not required to satisfy this principle, hence the sum of the mutual information of a given site with the remaining of the lattice is in general not bounded. Such a feature however does not affect the change of C_R at QPTs. C_R compares the two-point correlations ($Q2 + C2$) of the site i with its total correlations, that, in our case, are purely quantum ($Q2 + QS$). As we shall show, it is a useful tool to characterize the phase transitions $II \rightarrow I, III, IV$ in terms of two-point versus shared correlations.

IV. RESULTS AND DISCUSSION

In this section we first derive in the $\mu - u$ setting the results achieved by the method presented in 10 about the two-point/multipartite nature of the entanglement involved at each transition for the model Hamiltonian H_{BC} . We then deepen

the analysis by employing the measures described above (11), (17), (19) at the same transitions.

The method described in paragraph III A, classifies the type of entanglement involved at a given QPT by direct comparison of the derivatives of \mathcal{S}_i and \mathcal{I}_{ij} . In order to evaluate these two quantities the eigenvalues of the reduced density matrix ρ_i , and ρ_{ij} are needed. While the on-site reduced density matrix (II B) is already diagonal, the two-site density matrix (II B) is block diagonal and its eigenvalues $\tilde{\rho}_{ij}$ read

$$\tilde{\rho}_{ij} = \text{diag}\{D_1, \mathcal{O}_+, \mathcal{O}_-, D_2, \mathcal{P}_+, \mathcal{P}_-, \mathcal{Q}_+, \mathcal{Q}_-, D_3\}, \quad (20)$$

where, in the thermodynamic limit (TDL):

$$\mathcal{O}_\pm = (1-c) \left[n_s(1-n_s) + |\Gamma_{ij}| (|\Gamma_{ij}| \pm 1) \right], \quad (21)$$

$$\mathcal{Q}_+ = 2c(1-c) \left[(1-n_s)^2 - |\Gamma_{ij}|^2 \right], \quad (22)$$

$$\mathcal{Q}_- = 0, \quad (23)$$

$$\mathcal{P}_\pm = c \left[n_s(1-n_s) + |\Gamma_{ij}| (|\Gamma_{ij}| \pm 1) \right]. \quad (24)$$

In Tab. (II) we summarize the behaviour of the various functionals evaluated at the transition points. The method exposed in 10 allows one to identify two groups of QPTs. In the last column the transition is labelled as *Q2* whenever the divergencies displayed by $\partial_x \mathcal{S}_i$ and $\partial_x \mathcal{I}_{ij}$ are of the same type. In the other cases *i.e.*, when only $\partial_x \mathcal{S}_i$ displays a divergency, the transitions are labelled *QS*. As already discussed in Sec. III A, the two groups reflect the relevance and the role of the *Q2* and the *QS* correlations at the different transitions. The detailed analysis carried on in the following sections not only fully confirms the existence of these two groups, but also gives evidence of a further unexpected critical phenomenon occurring at each of the transition of *Q2* type.

A first consideration about Tab. II is in order. As already mentioned, we consider the derivatives with respect to u and μ which are the quantities that parameterize the Hamiltonian (1). At variance with the study in the $u - n$ setting developed in 10, the transition $I, I' \rightarrow IV$ is here described by $\partial_\mu \mathcal{S}_i$ and $\partial_\mu \mathcal{I}_{ij}$. This allows us to properly include it in the *Q2* group.

	$\partial_x \mathcal{S}_i$	$\partial_x \mathcal{I}_{ij}$	$\partial_x \mathcal{N}_{ij}$	$\partial_x \mathcal{C}_{ij}$	R_N	$\partial_x E_R$	Ent
$I, I' \rightarrow IV(x = \mu)$	$1/\sqrt{ \mu - \mu_c }$	$1/\sqrt{ \mu - \mu_c }$	$-1/\pi^2$	$1/\sqrt{ \mu - \mu_c }$	$1/\sqrt{ \mu - \mu_c }$	$1/\sqrt{ \mu - \mu_c }$	<i>Q2</i>
$II \rightarrow I, I'(x = u)$	$\log(u_c - u)$	f.	f.	-	f.	-	<i>QS</i>
$II \rightarrow III(x = u)$	$1/\sqrt{u - u_c}$	$1/\sqrt{u - u_c}$	$1/(2\pi^2)$	-	$1/\sqrt{u - u_c}$	-	<i>Q2</i>
$II \rightarrow IV(x = u)$	$1/\sqrt{u_c - u}$	$1/\sqrt{u_c - u}$	$-1/(4\pi^2)$	-	$1/\sqrt{u_c - u}$	-	<i>Q2</i>

TABLE II: Behaviour of R_N and the evaluated partial derivatives at the various QPTs (left column): the critical values u_c and μ_c can be inferred from table (I). 'f.' stands for finite value.

A. Two-point entanglement at *Q2* transition points

In this section we analyze the behaviour of the two-point correlations at each of the *Q2* transitions. We first proceed to the computation of the Negativity (11). At variance with the Concurrence, the Negativity can be used even when the local subsystem's Hilbert space has dimension greater than two, *i.e.* region *II*. We apply the partial transposition to ρ_{ij} , and then we proceed with its diagonalization. $\rho_{ij}^{T_i}$ is block diagonal and the only non diagonal sub-block reads

$$\begin{pmatrix} D_1 & O_2 & Q \\ O_2 & D_2 & P_2 \\ Q & P_2 & D_3 \end{pmatrix}. \quad (25)$$

The negative eigenvalues of $\rho_{ij}^{T_i}$ coincide with the negative eigenvalues of this sub-block. In the TDL the only possibly negative eigenvalue reads

$$\lambda_- = \frac{1}{2} \left[aP_{ij} + D_2 - \sqrt{[aP_{ij} - D_2]^2 + 4a|\Gamma_{ij}|^2} \right], \quad (26)$$

with $a = c^2 + (1-c)^2$. A straightforward calculation shows that

$$\mathcal{N}_{ij} = \begin{cases} -\lambda_- & \gamma_-^2 < \Gamma_{ij}^2 < \gamma_+^2, \\ 0 & \text{otherwise} \end{cases}, \quad (27)$$

$$\text{where } \gamma_\pm^2 = [1 - n_s(1 - n_s)] \pm \sqrt{1 - 2n_s(1 - n_s)}.$$

Quite interestingly, the result shows that the region characterized by non-vanishing Negativity, *i.e.* $\Gamma_{ij}^2 \in [\gamma_-^2, \gamma_+^2]$, depends only on n_s . Such a result reveals that the presence of *Q2* correlations in the TDL is deeply connected with the presence of the fermionic Sutherland Specie: when the latter is absent, all Negativities go to zero, whereas when $n_s \neq 0$ the relative number of empty or doubly occupied sites does not influence the presence of two-point entanglement.

1. Concurrence versus Negativity

Before proceeding in our analysis of the behavior of *Q2* correlations at the transition points, it is useful to compare

results obtained through Negativity (27) with those obtained with Concurrence (10) in the regions where the latter can be evaluated, *i.e.* regions *I* and *III*. As we shall see, even though it has been proven that both are measures of entanglement for qubits systems, the comparison show that in general they have different behavior and derivatives. As far as phase *I* is concerned we have that the Concurrence is given by

$$\mathcal{C}_{ij}^I = 2 \max \left\{ 0, |\Gamma_{ij}| - \sqrt{[(1-n)^2 - |\Gamma_{ij}|^2] (n^2 - |\Gamma_{ij}|^2)} \right\} , \quad (28)$$

whereas, specializing (27) to the case of region I , we obtain

$$\mathcal{N}_{ij}^I = \max \left\{ 0, \frac{1}{2} \left[(1-n)^2 + n^2 - 2|\Gamma_{ij}|^2 - \sqrt{(1-2n)^2 + 4|\Gamma_{ij}|^2} \right] \right\}. \quad (29)$$

Fig. 2–3 show that—as expected—both measures are non-vanishing in the same intervals (see (27)). Indeed, for $r = |i - j| > 1$ they start to differ from zero in correspondence of the same values of μ .

When both Concurrence and Negativity are non-zero, their behavior differs for at least two relevant aspects. First, apart from the case $r = 1$, the two quantities reach their maximum in correspondence of two different values of μ . Such a feature is compatible with the fact that in general the two measures provide a different ordering of the states²¹. Second, they differ in the behaviour of their derivatives with respect to μ . In particular, while at transition $I \rightarrow IV$ the derivative of Concurrence does display the correct diverging behavior ($\partial_\mu \mathcal{C}_{ij} \approx 1/\sqrt{|\mu_c - \mu|}$), $\partial_\mu \mathcal{N}_{ij}$ does not display any divergence.

As for region *III*, in the TDL both \mathcal{N}_{ij} and \mathcal{C}_{ij} are always

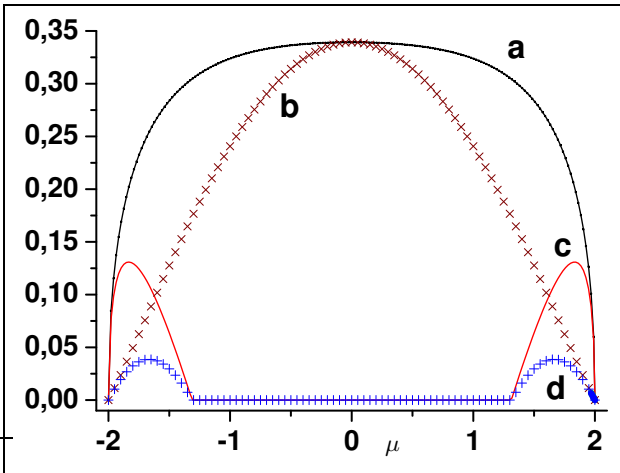


FIG. 2: Region I , $u > 4$. $\mathcal{N}_r, \mathcal{C}_r$ for $r = 1, 2$

zero. The behavior of the two quantities significantly differs if finite-size effects are included. Indeed, to first order in $1/L$ and for all $|i - j|$ the Concurrence reads

$$\mathcal{C}_{ij}^{III} = \begin{cases} \frac{1}{L} & n_d \neq 0, \\ 0 & \text{otherwise.} \end{cases} \quad (30)$$

while the Negativity is¹⁰

$$\mathcal{N}_{ij}^{III} = \frac{n_d(1-n_d)}{n_d^2 + (1-n_d)^2} \frac{1}{L} \quad . \quad (31)$$

2. Divergence of the Entanglement Range

The fact that \mathcal{N}_{ij} differs from zero at different values of μ depending on $|i - j|$ allows one to identify the Range of Negativity

$$R_{\mathcal{N}}(u, \mu) = \{r \mid \mathcal{N}_{i, i+r} \neq 0 \wedge \mathcal{N}_{i, i+r+1} = 0\}$$

i.e., the maximum distance r at which the Negativity is non-vanishing at fixed u, μ . We find that $R_{\mathcal{N}}$ is always finite but in the two following situations:

- when $n_s \rightarrow 0$ (transition $II \rightarrow III$);
- when $n_s \rightarrow 1$ (transitions $I \rightarrow IV$ and $II \rightarrow IV$) , in which R_N diverges.

In particular, $R_{\mathcal{N}}$ remains finite in correspondence of the two transitions $II \rightarrow I$, at which $n_s \rightarrow n \neq 1$ (and correspondingly $u \rightarrow u_c(n)$). In these cases only the nearest neighbor Negativity is always positive, *i.e.*, $R_{\mathcal{N}} \geq 1$. The condition that fixes the value of $R_{\mathcal{N}}$ is again $\Gamma_{ij}^2 = \gamma_-^2$.

The Entanglement Range allows one to better characterize the difference between $Q2$ and QS transitions. In the latter, the generic site i is correlated – via two-point quantum correlations – only with a finite number of neighboring sites, whereas, at $Q2$ transitions, the two-point quantum correlations begin to spread along the chain and, at the critical point, two arbitrarily distant sites are quantum correlated. This latter case is shown in Fig. 3 for the transition $I \rightarrow IV$, at which C_{ij} can be evaluated as well.

We can further characterize the spreading of the correlations

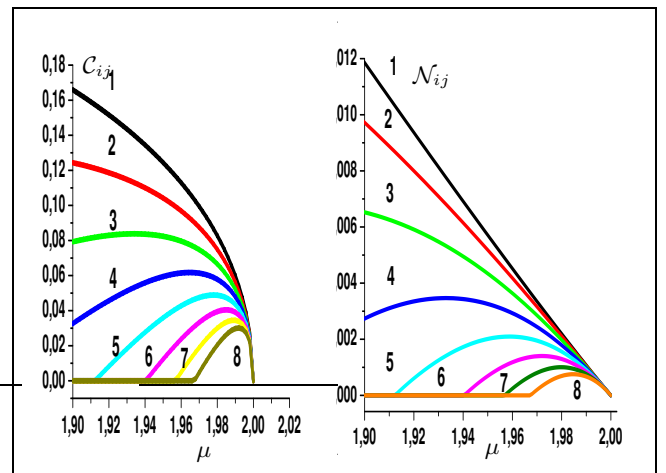


FIG. 3: Region I , $u > 4$. \mathcal{N}_{ij} (left) and \mathcal{C}_{ij} (right) for $r = 1, \dots, 8$

by analytically exploring the scaling behavior of R_N at the

transitions. We have that

$$R_N \approx \begin{cases} \frac{R_0}{n_s} & n_s \rightarrow 0 \\ \frac{R_0}{1-n_s} & n_s \rightarrow 1 \end{cases} \quad (32)$$

where $R_0 \approx 0.44$ is solution of

$$\frac{\sin \pi R_0}{\pi R_0} = \frac{1}{\sqrt{2}}. \quad (33)$$

The exponents ν_c characterizing the divergence of R_N at u_c and μ_c for the various transitions are easily worked out from (32) by recalling that n_s is a function of u and μ (see Tab. (I)). Quite interestingly, at all the three $Q2$ transitions we have:

$$\nu_c = \frac{1}{2} = \nu. \quad (34)$$

A similar type of behavior was already studied for a spin model⁷ where the notion of *entanglement transition* was introduced. In that case, the divergence of the Entanglement Range is observed for the Concurrence at some specific point of the phase diagram for which the ground state becomes factorized, and apparently no QPT takes place. We recognize such a feature for the model discussed here only in part. In fact here all the entanglement transitions occur in correspondence of QPTs; moreover, while phase IV is indeed characterized by a factorized structure (the ground state being singly occupied at each site), phase III is not, since the ground state in this phase is a superposition of empty and doubly occupied states distributed over the whole chain. This observation suggests the conjecture that a factorized structure with respect to Hilbert space appearing in the ground state is a *sufficient* but not necessary condition for the occurrence of an entanglement transition. The conjecture could also be generalized in terms of bipartite-entanglement: an entanglement transition occurs *iff* the new phase is a *two-point entanglement free* one. In this sense the factorized state of phase IV and the genuine multipartite ground state of phase III are equivalent. Moreover, at least in our model, it is equivalent the way in which the system destroys all correlations (IV) or build genuine multipartite ones (III).

B. Two-point versus multipartite entanglement at QPTs

In order to explore the role of multipartite entanglement at the various transitions an ideal tool would be the Entanglement Ratio E_R (17), which, as explained, provides a direct measure of the relative role of $Q2$ and QS : a decreasing (increasing) Entanglement Ratio in proximity of a QPT means that QS ($Q2$) correlations are more relevant to the transition. According to (16) τ_2 is properly measured through Concurrence. This implies that only the transitions in which the system is of qubit nature (namely, the $I \rightarrow IV$ transition) can be explored through E_R , whereas in region II we used the (below described) Correlation Ratio.

1. Entanglement Ratio

We start exploring the behavior of E_R in phase I –where \mathcal{C}_{ij} is defined– and in particular at the transition $I \rightarrow IV$. As far as τ_1 is concerned, from (16) we have

$$\tau_1^I = 4 \det [\rho_i^I] = 4n(1-n). \quad (35)$$

As for τ_2 , the two-site Concurrence was given in (28); still, the evaluation of the sum of the $(L-1) \mathcal{C}_{ij}^2$ in (16) requires some effort. In fact, \mathcal{C}_{ij} depends on the distance r between the two sites; one has first evaluate the sum

$$\tau_2(N_s, L) = \sum_{r=1}^{L-1} \mathcal{C}_r^2(N_s, L) \quad (36)$$

and then the TDL $\lim_{N_s, L \rightarrow \infty} \tau_2(N_s, L)$. The numerical evaluation of E_R for a sufficiently large r is reported in Fig. 4. The latter clearly shows that, as expected, in the vicinity of

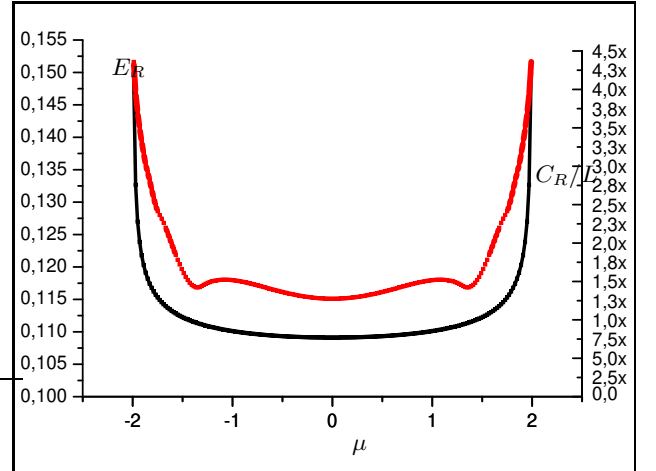


FIG. 4: Region I , $u > 4$. Entanglement ratio E_R and normalized Correlation Ratio C_R/L with $L = 1000$.

transition $I \rightarrow IV$ ($\mu \rightarrow 2$) the $Q2$ correlations rapidly increase with respect to QS ones. We notice that interestingly the derivative of r diverges again with $\sqrt{|\mu - 2|}$ at the transition.

We then pass to explore τ_2 in region III , which is again of qubit nature. Since such a region is characterized by the presence of just η -pairs, which have an intrinsic multipartite nature, we expect that E_R to vanish there. As far as τ_1 is concerned we have that:

$$\tau_1^{III} = 4 \det [\rho_i^{III}] = 4n_d(1-n_d), \quad (37)$$

whereas for τ_2 one can see that, since $\mathcal{C}_{ij}^{(III)} \tilde{1} - L$ (see (30)) is independent on r and vanishing in the TDL, $\tau_2 = \sum_j \mathcal{C}_{ij}^2 = 0$. Hence, the Entanglement Ratio correctly indicates that *the only relevant entanglement is multipartite* (i.e. n -way entanglement with $n \geq 3$).

2. QS correlations in region II

As a general fact, in region *II* both *Q2* and *QS* correlations are present. In particular, the *QS* transitions –which according to Tab. (II) are $II \rightarrow I, I'$ at fixed u – should be characterized by some change in multipartite entanglement *QS*. Such an hypothesis has a first strong confirmation in the fact that at these transitions η -pairs (and ODLRO, see (5)) disappear. Indeed, it has been shown in 30 that η -pairs do carry multipartite entanglement, thus disappearing at these transitions. Furthermore, the behavior of *Q2* correlations is here radically different from the one they display at *Q2* transitions. Actually, as already seen in paragraph (IV A 2) the Entanglement Range is finite at any $\mu \in [-2, 2]$ for $u \leq u_c(n)$; moreover both R_N and \mathcal{N}_{ij} , and their derivatives remain finite in the same regime.

At $\mu = 2$ (i.e., at transition $II \rightarrow IV$) –besides *QS*– also *Q2* correlations enter to play a role. In fact, while η -pairs disappear, R_N becomes infinite and an entanglement transition takes place. Since the analysis of previous section has shown that R_N has the same divergence of \mathcal{S}_i , we infer that the role of *Q2* correlations is dominant at this transition. In order to confirm such a scheme we now use the Correlation Ratio previously introduced.

3. Correlation Ratio

We aim at obtaining an indicator of the relative weight of *Q2* correlations with respect to *QS* ones in region *II*. Since \mathcal{I}_{ij} keeps track of the change of *Q2* correlations between i and j at transition points, we expect that the Correlation Ratio C_R (19), to capture such a desired feature.

We first consider the behavior of C_R in region *I*, where it can be compared with the standard Entanglement Ratio E_R ; this is shown for sufficiently large L by the dashed line in Fig. 4. In correspondence of the transition $II \rightarrow IV$ C_R correctly reproduces the qualitative behavior of E_R i.e., the relative weight of *Q2* correlations rapidly increase.

In Fig. 6 we report $C_R(u)$ in region *II* at two different values of n ($n = 1/2$ and $n = 1$). At both values C_R rapidly increases in proximity of $u = -4$ (transition $II \rightarrow III$). The behavior of C_R is quite different in the two cases in correspondence of the upper critical point. Indeed, for $n = 1/2$ ($II \rightarrow I$) it goes to zero with a clear linear dependence on $u_c - u$, reminiscent of the behavior of the pairing gap Δ_P . Whereas for $n = 1$ (transition $II \rightarrow IV$) –after decreasing in almost the whole region– C_R rapidly increases for $u \rightarrow 0$.

These features are in accordance with the considerations exposed in the previous paragraph. Whenever C_R increases at the transition, this implies that *Q2* correlations are increasing with respect to *QS*, and hence the transition should be of *Q2* type. On the other hand, it is only at the transition of *QS* type (transition $II \rightarrow I$) that C_R vanishes, meaning that *QS* correlations overcome *Q2* ones.

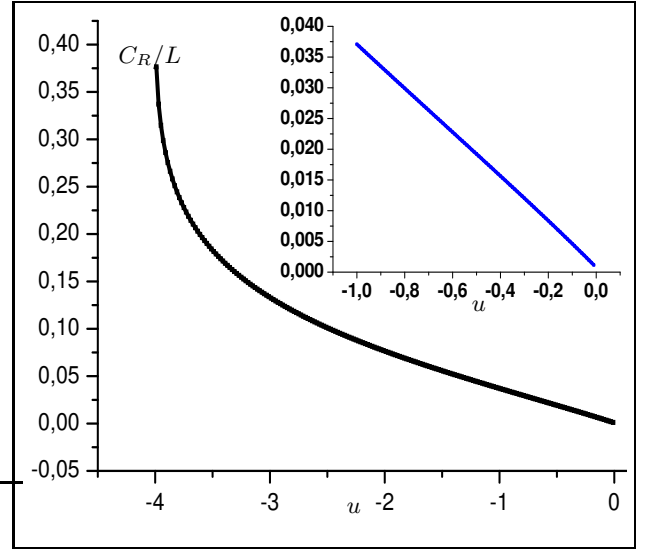


FIG. 5: Region *II*, $n = 1/2$ $u \in [-4, 0]$. Normalized Correlation Ratio C_R/L with $L = 1000$. Inset: zoom of the transition $II \rightarrow I$

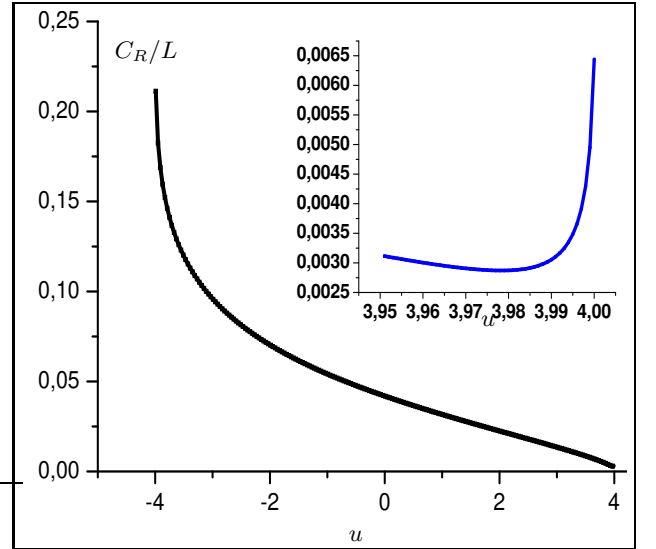


FIG. 6: Region *II*, $n = 1$, $u \in [-4, 4]$. Normalized Correlation Ratio C_R/L with $L = 1000$. Inset: zoom of the transition $II \rightarrow IV$

C. Entanglement away from QPTs

Apart from transition points, we can spot the areas in the different regions where the *QS* correlations prevail with respect to *Q2* correlations from the direct study of $\mathcal{S}_i, \mathcal{N}_{ij}$. In Region *III*, *QS* prevail everywhere since \mathcal{S}_i is different from zero and all \mathcal{N}_{ij} are vanishing. Let us recall that one has genuine multipartite entanglement whenever both $\mathcal{S}_i \neq 0$ and two-point entanglement is zero. Here it is due to the presence of η -pairs, which is also captured by two-point classical correlations. In fact it turns out that $\mathcal{I}_{ij}^{(III)} = \mathcal{I}_{\infty}^{(III)} = 2n_d(1 - n_d) \forall j$, with $\mathcal{I}_{\infty} \doteq \lim_{|i-j| \rightarrow \infty} \mathcal{I}_{|i-j|}$. All pairs of sites are equally correlated as two infinitely distant sites.

Interestingly this property is directly related to the presence of ODLRO (see 5) in that the total amount of correlations is simply proportional to it.

In region I QS prevail away from transition points since the Entanglement Ratio has a minimum (see Fig. 4). Contextually only the nearest neighbor Negativity is nonzero, and S_i is maximum; moreover $\mathcal{I}_{\infty}^{(I)} = 0$.

The same qualitative behavior holds inside region II as well, except that $\mathcal{I}_{\infty}^{(II)} \neq 0$ in the whole region but at transition $II \rightarrow I$, as can be seen from the dashed line in Fig. 8. This is related with the fact that η -pairs are present in region II as well. Quite interestingly, the contribution of singly occupied and doubly occupied sites to two-point correlations seem to simply add in quantum mutual information. Indeed, one could check that, with amazing accuracy, $\mathcal{I}_{ij}^{(II)} \approx \mathcal{I}_{ij}^{(I)} + \mathcal{I}_{\infty}^{(II)}$.

To resume, we observe that an infinite range of two-point correlations in proximity of a transition is a signal of a $Q2$ -driven QPT, in which case also R_N diverges. Far from transition the same infinite range is implied whenever $\mathcal{I}_{\infty} \neq 0$ and it is thus a signal of the existing ODLRO, in our case related to η -pairs (see (5)).

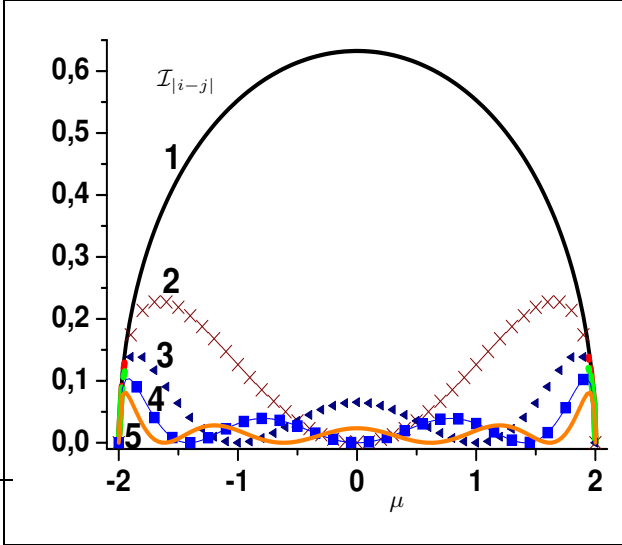


FIG. 7: Region I , $u > 4$. Mutual information \mathcal{I}_{ij} , $r = 1, \dots, 5$

V. CONCLUSIONS

In this paper we analyzed the rich phase diagram of the one-dimensional bond-charge extended Hubbard model at $T = 0$ by means of various measures of bipartite/multipartite correlations. All the computed measures allow one to reproduce the known phase diagram in terms of singularities; moreover, at each transition the critical exponent of the correlation length is shown to coincide with the scaling exponent of the divergent quantities, when evaluated.

As anticipated in 10, and proved here in details, the solely knowledge of one- and two-site Von Neumann entropy allows one to distinguish the quantum phase transitions (QPTs) in

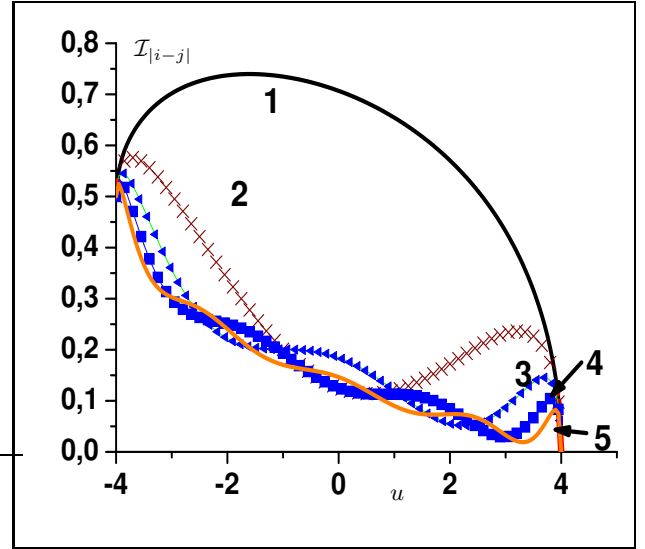


FIG. 8: Region II , $n = 1$ $u \in [-4, 4]$. Mutual information \mathcal{I}_{ij} , $r = 1, \dots, 5$

which the role of two-point quantum correlations ($Q2$) is relevant from those in which multipartite quantum correlations (QS) are determinant.

The systematic analysis of other known measures of entanglement at the different transitions and phases made it possible to better characterize both $Q2$ and QS transitions. Contextually a new estimator which can be computed for qudits systems has been introduced: the *Correlation Ratio*. The latter is an indicator of the relative weight of the two-point correlations with respect to the total (quantum) ones at the transitions.

The analysis shows that $Q2$ transitions are characterized by a divergence in the Range of Negativity: when approaching the transition two sites at arbitrary distance become quantum correlated. Such a feature is reflected in the behavior of the Entanglement/Correlation Ratio. The latter increases at $Q2$ critical points with diverging derivative, clearly indicating an increasing relative weight of two-point quantum correlations with respect to multipartite ones.

QS transitions instead are characterized by a finite Range of Negativity and by a vanishing Correlation Ratio, indicating that multipartite quantum correlations dominate there. For our model, the correlated physical phenomenon is the disappearance of η -pairs.

Finally, we described the nature of the correlations within each region as well. For our model, the existence of two-point quantum correlations depends only on the presence of singly occupied sites. At the same time, the presence of doubly occupied sites witnesses the appearance of η -pairs and ODLRO, and multipartite entanglement carried by them. ODLRO reflects as well at the level of two-point correlations as a finite value of quantum mutual information between infinitely distant sites.

In conclusion, the above analysis has widely clarified how to characterize the nature of quantum correlations involved at a QPT for an integrable correlated electrons model. The scheme in particular allows to gain from quantum mutual in-

formation insight on the behavior of both Q2 and QS correlations at transition points for $T = 0$.

There is no reason to expect that the output of the scheme would change away from integrability, either in one or in greater dimension. A first step in this direction has been achieved in one dimension by means of the numerical analysis in the non-integrable case (1)¹².

It remains to be investigated how modifying the proposed scheme at $T \neq 0$, where also temperature driven correlations play a major role; in particular, it is expected they would compete with quantum ones in determining the behavior of quantum mutual information.

APPENDIX A: REDUCED DENSITY MATRIX EXPANSION

Let us recall the definition of the reduced density matrix ρ_{ij} :

$$\rho_{ij} = \text{Tr}_{L/ij} |\Psi_{GS}\rangle\langle\Psi_{GS}|; \quad (\text{A1})$$

given that the pure state $|\Psi_{GS}\rangle$ can be written as

$$|\Psi_{GS}\rangle = \sum_{ab} C_{ab} |a\rangle|b\rangle, \quad C_{ab} \in \mathbb{C}, \quad (\text{A2})$$

where $\{|a\rangle\}$ and $\{|b\rangle\}$ are basis for the subsystem $\{ij\}$ and $\{L/ij\}$ respectively, the operator expansion for ρ_{ij} is easily derived:

$$\begin{aligned} \rho_{ij} &= \text{Tr}_{L/ij} \sum_{aa'bb'} C_{ab} C_{a'b'}^* |a\rangle|b\rangle\langle b'| \langle a'| \\ &= \sum_{aa'bb'b''} C_{ab} C_{a'b'}^* \langle b''|a\rangle|b\rangle\langle b'| \langle a'|b''| \\ &= \sum_{aa'bb'b''} C_{ab} C_{a'b'}^* (-)^{(ab+a'b')} |a\rangle\langle a'| \delta_{bb''} \delta_{b'b''} \\ &= \sum_{aa'b} C_{a'b}^* (-)^{(a+a')b} |a\rangle\langle a'| \\ &= \sum_{aa'} C_{aa'} |a\rangle\langle a'|, \end{aligned} \quad (\text{A3})$$

where

$$C_{aa'} = \sum_b C_{ab} C_{a'b}^* = \langle \Psi_{GS} | a \rangle \langle a' | \Psi_{GS} \rangle, \quad (\text{A4})$$

where $(-)^a$ takes into account the parity of the state $|a\rangle$ ¹⁷. It turns out that for our model $a + a' = 0$ for all (a, a') , due to the conservation of N_s and N_d .

APPENDIX B: DIMER REDUCED DENSITY MATRIX EVALUATION

In this section we schematically give the procedures to compute the dimer reduced density-matrix. The mean value of the following operators give the diagonal elements of ρ_{ij} :

$$\begin{aligned} X_i^{02} X_i^{20} X_j^{02} X_j^{20}, \quad X_i^{02} X_i^{20} X_j^{11}, \quad X_i^{11} X_j^{02} X_j^{20}, \\ X_i^{11} X_j^{11}, \quad X_i^{11} X_j^{22}, \quad X_i^{22} X_j^{11}, \\ X_i^{02} X_i^{20} X_j^{22}, \quad X_i^{22} X_j^{02} X_j^{20}, \quad X_i^{22} X_j^{22}. \end{aligned} \quad (\text{B1})$$

Due to the conservation of N_s and N_d , the only off-diagonal elements that can be non-vanishing in some of the regions are the following ones (together with their Hermitian conjugates)

$$X_i^{10} X_j^{01}, \quad -X_i^{21} X_j^{12}, \quad X_i^{02} X_j^{20}. \quad (\text{B2})$$

The action of the latter is simply to permute the states on the two sites.

a. Region I

Since the ground state in region I is given by a superposition of states in which each site is empty or singly occupied and since $N_s = N_{tot} \doteq N$, and $X_i^{02} X_i^{20} \equiv [1 - X_i^{11}]$ the only non-zero entries are given by:

$$\begin{aligned} \langle X_i^{02} X_i^{20} X_j^{02} X_j^{20} \rangle_I &\equiv \langle (1 - X_i^{11})(1 - X_j^{11}) \rangle_I, \\ \langle X_i^{02} X_i^{20} X_j^{11} \rangle_I &\equiv \langle (1 - X_i^{11}) X_j^{11} \rangle_I, \\ \langle X_i^{11} X_j^{02} X_j^{20} \rangle_I &\equiv \langle X_i^{11} (1 - X_j^{11}) \rangle_I, \end{aligned} \quad (\text{B3})$$

and

$$\langle X_i^{11} X_j^{11} \rangle_I, \quad \langle X_i^{10} X_j^{01} \rangle_I; \quad (\text{B4})$$

where $\langle \mathcal{O} \rangle_I \equiv \langle \Psi_I(N, L) | \mathcal{O} | \Psi_I(N, L) \rangle$. We thus compute $\langle X_i^{11} \rangle_I$ using the expression of both $|\Psi_I(N, L)\rangle$ and X_i^{11} in terms of momentum operators

$$\langle X_i^{11} \rangle_I = \frac{1}{L} \sum_{k, k'} \exp[i(k - k')j] \langle \tilde{X}_k^{10} \tilde{X}_{k'}^{01} \rangle_I = \frac{N}{L}, \quad (\text{B5})$$

since the only non-vanishing terms of the sum in (B5) are those for which $k - k' = 0$.

The calculation of $\langle X_i^{10} X_j^{01} \rangle_I$ is analogous to the previous one; here we have the appearance of a phase factor:

$$\langle X_i^{10} X_j^{01} \rangle_I = \frac{1}{L} \sum_m \exp[-i2\pi m(i - j)/L] \doteq \Gamma_{i-j} \quad (\text{B6})$$

Such a phase factor has different expression for N even or odd:

$$|\Gamma_{i-j}^E| = |\Gamma_{i-j}^O| = \frac{\sin(\frac{N}{L}\pi|i - j|)}{L \sin(\frac{1}{L}\pi|i - j|)}. \quad (\text{B7})$$

In the TDL, $\Gamma_{ij} = \Gamma_{ij}^E = \Gamma_{ij}^O$ and it can be computed by approximating the sum in (B6) with the following integral

$$\Gamma_{ij} = \frac{1}{\pi} \int_0^{m\pi} \cos k(i - j) dk = \frac{\sin(n|i - j|\pi)}{\pi|i - j|}. \quad (\text{B8})$$

The previous calculations allow us to eventually compute

$$\langle X_i^{11} X_j^{11} \rangle_I = \left(\frac{N}{L} \right)^2 - \Gamma_{i-j} \Gamma_{j-i}. \quad (\text{B9})$$

The expressions of D_1 , D_2 , O_1 , O_2 in region I ($N_d = 0$) follow from the collection of the previous results.

b. Region III

The ground state in region *III* is given by a superposition of states in which each site is empty or doubly occupied. The only non-zero entries are given by

$$\begin{aligned} & \langle X_i^{02} X_i^{20} X_j^{02} X_j^{20} \rangle_{III}, \quad \langle X_i^{02} X_i^{20} X_j^{22} \rangle_{III}, \\ & \langle X_i^{22} X_j^{02} X_j^{20} \rangle_{III}, \end{aligned} \quad (\text{B10})$$

and

$$\langle X_i^{22} X_j^{22} \rangle_{III}, \quad \langle X_i^{02} X_j^{20} \rangle_{III}, \quad (\text{B11})$$

where $\langle \mathcal{O} \rangle_{III} \equiv \langle \Psi_{III}(N, L) | \mathcal{O} | \Psi_{III}(N, L) \rangle$. The evaluation of (B10) follows from the evaluation of (B11). A general strategy is used. In the case of $\langle X_i^{22} X_j^{22} \rangle_{III}$ one has to count the number of states in the superposition $|\Psi_{III}(N, L)\rangle$ whose sites i and j are doubly occupied:

$$\langle X_i^{22} X_j^{22} \rangle_{III} = N_{III}(N_d) \binom{L-2}{N_d-2} = \frac{N_d(N_d-1)}{L(L-1)} \quad (\text{B12})$$

In order to compute $\langle X_i^{02} X_j^{20} \rangle_{III}$ one has to count all the states whose site i is doubly occupied and whose site j is empty. This leads to the following result

$$\langle X_i^{02} X_j^{20} \rangle_{III} = N_{III}(N_d) \binom{L-2}{N_d-1} = \frac{N_d(L-N_d)}{L(L-1)} \quad (\text{B13})$$

The expressions of D_1, D_3, Q in region *III* ($N_s = 0$) follow from the previous results.

c. Region II

We start by noticing that since $[X_i^{11}, \eta^\dagger] = 0$ the operator X_i^{11} does not affect the doubly occupied part of the ground state. Accordingly:

$$\begin{aligned} \langle N_d | X_i^{11} | N_d \rangle_{II} &= \frac{N_s}{L}, \\ \langle N_d | X_i^{11} X_j^{11} | N_d \rangle_{II} &= \left(\frac{N_s}{L} \right)^2 - |\Gamma_{i-j}|^2; \end{aligned}$$

where the notation $\langle N_d | \mathcal{O} | N_d \rangle_{II} \equiv \langle \Psi_{II}(N_s, N_d, L) | \mathcal{O} | \Psi_{II}(N_s, N_d, L) \rangle$ will be useful in the following calculations.

We now compute $\langle N_d | X_j^{22} | N_d \rangle$. In a first step we make use of the following relations

i) $[X_j^{22}, (\eta^\dagger)^{N_d}] = N_d(\eta^\dagger)^{N_d-1} X_j^{20}$;

ii) $[X_j^{20}, (\eta^\dagger)^{N_d-1}] = 0$;

iii) $(\eta)^{N_d} = (\eta)^{N_d-1} \eta$.

The latter imply that

$$\begin{aligned} & [N_{II}(N_d)]^2 \langle \Psi_I | (\eta)^{N_d} X_j^{22} (\eta^\dagger)^{N_d} | \Psi_I \rangle \\ &= [N_{II}(N_d)]^2 N_d \langle \Psi_I | (\eta)^{N_d} (\eta^\dagger)^{N_d-1} X_j^{20} | \Psi_I \rangle \\ &= \frac{[N_{II}(N_d)]^2}{[N_{II}(N_d-1)]^2} N_d^2 \langle N_d-1 | X_j^{02} X_j^{20} | N_d-1 \rangle. \end{aligned}$$

If we now define $\mathcal{D}_{N_d-1} \doteq \langle N_d-1 | X_j^{02} X_j^{20} | N_d-1 \rangle$, we may write the following recursive equation:

$$\mathcal{D}_{N_d} = 1 - \frac{N_s}{L} - \frac{N_d}{L-N_s-N_d+1} \mathcal{D}_{N_d-1}, \quad (\text{B14})$$

whose solution is $\mathcal{D}_{N_d} = \frac{L-N_s-N_d}{L}$. Thus, by collecting the above results, we have

$$\langle N_d | X_j^{22} | N_d \rangle = \frac{[N_{II}(N_d)]^2}{[N_{II}(N_d-1)]^2} N_d^2 \mathcal{D}_{N_d-1} = \frac{N_d}{L}. \quad (\text{B15})$$

We now compute $\langle N_d | X_i^{11} X_j^{22} | N_d \rangle$ by resorting to the solution of a recursive equation. Since $[X_j^{22}, X_i^{11}] = 0$ we can first apply the procedure used for $\langle N_d | X_j^{22} | N_d \rangle$ to obtain

$$\langle N_d | X_j^{22} X_i^{11} | N_d \rangle = \frac{[N_{II}(N_d)]^2}{[N_{II}(N_d-1)]^2} (N_d)^2 \mathcal{E}_{N_d-1}, \quad (\text{B16})$$

where $\mathcal{E}_{N_d-1} \doteq \langle N_d-1 | X_j^{02} X_j^{20} X_i^{11} | N_d-1 \rangle$ satisfies the following recursive expression

$$\begin{aligned} \mathcal{E}_{N_d-1} &= \langle N_d-1 | (1 - X_j^{11}) X_i^{11} | N_d-1 \rangle \\ &\quad - \frac{[N_{II}(N_d-1)]^2}{[N_{II}(N_d-2)]^2} (N_d-1)^2 \mathcal{E}_{N_d-2} \\ &= \frac{N_s}{L} - \frac{N_s^2}{L^2} + |\Gamma_{i-j}|^2 \\ &\quad - \frac{N_d-1}{L-N_s-N_d+2} \mathcal{E}_{N_d-2}. \end{aligned} \quad (\text{B17})$$

The solution of the latter is

$$\mathcal{E}_{N_d} = \left(1 - \frac{N_d}{L-N_s} \right) \left[\frac{N_s}{L} \left(\frac{L-N_s}{L} \right) + |\Gamma_{i-j}|^2 \right] \quad (\text{B18})$$

and, finally, we get

$$\langle N_d | X_j^{22} X_i^{11} | N_d \rangle = \frac{N_d}{L-N_s} \left[\frac{N_s(L-N_s)}{L^2} + |\Gamma_{i-j}|^2 \right] \quad (\text{B19})$$

We now compute $\langle N_d | X_i^{22} X_j^{22} | N_d \rangle$. The same arguments used for (B17) lead to

$$\langle N_d | X_j^{22} X_i^{22} | N_d \rangle = \frac{[N_{II}(N_d)]^2}{[N_{II}(N_d-2)]^2} N_d^2 (N_d-1)^2 \mathcal{F}_{N_d} \quad (\text{B20})$$

where the function defined as $\mathcal{F}_{N_d} \doteq \langle N_d | X_j^{02} X_j^{20} X_i^{02} X_i^{20} | N_d \rangle$ satisfies the following recursive equation:

$$\mathcal{F}_m = (\alpha - \alpha') \left(1 - \frac{m}{\beta} \right) - \frac{m}{\beta - m + 1} \mathcal{F}_{m-1} \quad (\text{B21})$$

with

$$\begin{aligned} \alpha &= 1 - \frac{N_s}{L}, & \beta &= L - N_s, \\ \alpha' &= \frac{N_s}{L} - \frac{N_s^2}{L^2} + |\Gamma_{i-j}|^2, & m &= N_d. \end{aligned} \quad (\text{B22})$$

The latter recursive equation is solved by defining the auxiliary function $\mathcal{G}_m \doteq \frac{m}{\beta-m+1} \mathcal{F}_{m-1} \frac{1}{(\alpha-\alpha')}$, that obeys

$$\mathcal{G}_m = \frac{m}{\beta} - \frac{m}{\beta - m + 1} \mathcal{G}_{m-1}, \quad (\text{B23})$$

whose solution is $G_m = -\frac{m(\beta-m)}{\beta(\beta-1)}$. Collecting the above results we have that

$$\begin{aligned} & \langle N_d | X_j^{22} X_i^{22} | N_d \rangle \\ &= \frac{N_d(N_d-1) \left[\left(1 - \frac{N_s}{L}\right)^2 - |\Gamma_{i-j}|^2 \right]}{(L-N_s)(L-N_s-1)}. \end{aligned} \quad (\text{B24})$$

The computation of $\langle N_d | X_i^{02} X_j^{20} | N_d \rangle$ is now straightforward, since it can be expressed in terms of the above defined \mathcal{F}_m :

$$\begin{aligned} & \langle N_d | X_i^{02} X_j^{20} | N_d \rangle = \frac{[N_{II}(N_d)]^2}{[N_{II}(N_d-1)]^2} N_d^2 \mathcal{F}_{N_d-1} \\ &= \frac{N_d(L-N_s-N_d) \left[\left(1 - \frac{N_s}{L}\right)^2 - |\Gamma_{i-j}|^2 \right]}{(L-N_s)(L-N_s-1)}. \end{aligned} \quad (\text{B25})$$

The same argument holds for $\langle N_d | X_i^{02} X_i^{20} X_j^{22} | N_d \rangle$:

$$\begin{aligned} & \langle N_d | X_i^{02} X_i^{20} X_j^{22} | N_d \rangle = \frac{[N_{II}(N_d)]^2}{[N_{II}(N_d-1)]^2} N_d^2 \mathcal{F}_{N_d-1} \\ &= \langle N_d | X_j^{02} X_i^{20} | N_d \rangle. \end{aligned} \quad (\text{B26})$$

The previous steps allow us to easily evaluate $\langle N_d | X_i^{02} X_i^{20} X_j^{11} | N_d \rangle$ in terms of (B18):

$$\langle N_d | X_i^{02} X_i^{20} X_j^{11} | N_d \rangle = \mathcal{E}_{N_d}. \quad (\text{B27})$$

We then compute $\langle N_d | X_i^{10} X_j^{01} | N_d \rangle$. Using the following relations

i) $[X_i^{10} X_j^{01}, (\eta^\dagger)^{N_d}] = -N_d X_i^{10} X_j^{21} (\eta^\dagger)^{N_d-1}$;

ii) $(\eta)^{N_d} X_j^{21} = N_d (\eta)^{N_d-1} X_j^{01}$,

we obtain the recursive equation

$$\begin{aligned} \mathcal{L}(N_d) &\doteq \langle N_d | X_i^{10} X_j^{01} | N_d \rangle \\ &= \frac{N_d \mathcal{L}(N_d-1)}{N_d - L - N_s + 1} + \Gamma_{i-j}, \end{aligned} \quad (\text{B28})$$

whose solution is

$$\langle N_d | X_i^{10} X_j^{01} | N_d \rangle = \Gamma_{i-j} \frac{L - N_s - N_d}{L - N_s}. \quad (\text{B29})$$

The task of evaluating $\langle N_d | X_i^{12} X_j^{21} | N_d \rangle$ is simplified by observing that $[X_j^{10} X_i^{01}, \eta^\dagger] = [X_i^{21} X_j^{12}, \eta^\dagger]$; we obtain:

$$\begin{aligned} \langle N_d | X_i^{21} X_j^{12} | N_d \rangle &= (N_d)^2 \frac{[N_{II}(N_d)]^2}{[N_{II}(N_d-1)]^2} \mathcal{L}(N_d-1) \\ &= \frac{N_d}{L - N_s} \Gamma_{j-i}, \end{aligned} \quad (\text{B30})$$

where $\mathcal{L}(N_d-1)$ is given by (B28).

¹ M.A. Nielsen and I.L. Chuang, *Quantum Computation and Quantum Information* (Cambridge University Press, Cambridge, UK 2000).

² S.Sachdev, *Quantum Phase Transitions* (Cambridge University Press, Cambridge, UK 2000).

³ A. Osterloh, L. Amico, P. Falci, R. Fazio, *Nature (London)* **416**, 608 (2002);

⁴ T.J. Osborne and M.A. Nielsen, *Phys. Rev. A* **66**, 032110 (2002).

⁵ L. Wu, M. Sarandy, and D. A. Lidar, *Phys. Rev. Lett.* **93**, 250404 (2004)

⁶ T. Roscilde et al., *Phys. Rev. Lett.* **93**, 167203 (2004)

⁷ L. Amico et al., *Phys. Rev. A* **74**, 022322 (2006)

⁸ L. Campos Venuti, C. Degli Esposti Boschi, G. Morandi, et al., *Phys. Rev. A* **73** 010303 (2006)

⁹ S. Gu, S. Deng, Y. Li, H. Lin, *Phys. Rev. Lett.* **93**, 086402 (2004).

¹⁰ A. Anfossi, P. Giorda, A. Montorsi, et al. *Phys. Rev. Lett.* **95**, 056402 (2005)

¹¹ D. Larsson, and H. Johannesson, *Phys. Rev. Lett.* **95** 196406 (2005)

¹² A. Anfossi, C. Degli Esposti Boschi, A. Montorsi, and F. Ortolani, *Phys. Rev B* **73**, 085113 (2006)

¹³ B. Sutherland, *Phys. Rev. B* **12**, 3795 (1975)

¹⁴ L. Arrachea, and A.A. Aligia, *Phys. Rev. Lett.* **73**, 2240 (1994).

¹⁵ F. Dolcini, and A. Montorsi, *Phys. Rev. B* **66**, 075112 (2002).

¹⁶ L. Arrachea, A.A. Aligia, E. Gagliano, *Phys. Rev. Lett.* **76**, 4396-4399 (1996)

¹⁷ A. Anfossi, and A. Montorsi, *J. Phys. A: Math. Gen.* **38**, 4519 (2005)

¹⁸ J. I. Latorre, E. Rico, G. Vidal, *Quantum Inf. Comput.*, **4** 48 (2004); G. Vidal et al., *Phys. Rev. Lett.* **90**, 227902 (2003).

¹⁹ W. K. Wootters, *Phys. Rev. Lett.* **80**, 2245 (1998).

²⁰ G. Vidal and R. F. Werner *Phys. Rev. A* **65**, 032314 (2002).

²¹ F. Verstraete, K. Audenaert, J. Dehaene, B. De Moor, *J. Phys. A* **34**, 10327 (2001)

²² V. Coffman, J. Kundu, and W. K. Wootters, *Phys. Rev. A* **61**, 052306 (2000)

²³ T. J. Osborne, F. Verstraete, *Phys. Rev. Lett.* **96**, 220503 (2006)

²⁴ B. Groisman, S. Popescu, and A. Winter, *quant-ph/0410091*.

²⁵ A. Wong, N. Christensen, *Physical Review A* **63**, 044301 (2001)

²⁶ C. Yu, H. Song, *Phys. Rev. A* **71** 042331 (2005)

²⁷ V. Vedral, *Rev. Mod. Phys.* **74**, 197-234 (2002).

²⁸ P. Zanardi, *Phys. Rev. A* **65**, 042101 (2002); H. Fan, and S. Lloyd, *J. Phys. A* **38**, 5285 (2005).

²⁹ S. Lee et al., *Phys. Rev. A* **68**, 062304 (2003).

³⁰ V. Vedral, *New J. Phys.* **6**, 102 (2004).

³¹ Z. Sun et al., *Commun. Theor. Phys.* **43**, 1033 (2005).